SEE CORRECTION FOR THIS ARTICLE
PNAS RESEARCH ARTICLE | EVOLUTION
OPEN ACCESS

Competing models of hominin body size evolution

Jacob D. Gardner[a,1], Thomas A. Püschel[b], Suzy White[a,c], Manabu Sakamoto[a], and Chris Venditti[a,1]

Edited by Scott V. Edwards, Harvard University, Cambridge, MA; received August 8, 2025; accepted May 12, 2026

The evolutionary trajectory of hominin body size remains contested, with prior studies suggesting a gradual increase or lineage-specific shifts. Here, we apply Bayesian phylogenetic generalized linear mixed models to a dataset of 386 specimens across 21 taxa and find strong evidence for a marked body mass increase in non-*habilis* or later-occurring *Homo*, with moderate support for a general increase over time. Contrary to some existing hypotheses, we find less support for a distinct size increase across all *Homo*. By accounting for phylogenetic nonindependence, intraspecific variation, and multiple sources of uncertainty, our analysis examines competing views in a single framework, supporting a more complex explanation for hominin body size evolution and clarifying key transitions in *Homo*.

hominins | body mass | size | phylogenetic comparative methods

Significance

Despite its central role in hominin evolution, there is little consensus on how body size increased through time. Our study examines competing hypotheses concurrently in a mixed model framework, where we account for phylogenetic relationships, intraspecific variation, and multiple sources of data uncertainty. We provide strong evidence for a marked size increase in later-occurring *Homo*, alongside a moderate general increase over time among all hominins. By reconciling conflicting findings within a single framework, our results clarify key evolutionary transitions and highlight the complex nature of body size change in human evolution.

Body size is central to organismal biology, influencing ecology (1), life history (2), physiology (3), and neuroanatomy (4). In the context of hominin evolution, increases in body size have been linked to larger brains, improved bipedal locomotion, and expanded range sizes (5, 6). However, despite its importance, there is no consensus on whether hominin body size increased consistently over time (7–12).

Recent studies present conflicting views (Fig. 1). Some argue against a general evolutionary trend (9–11), while others support an overall increase in body mass and stature (12). Small-bodied taxa like *Homo floresiensis* and *Homo naledi* are often cited as exceptions (11, 12). Additionally, some researchers suggest that size increases may be specific to *Homo* (13) or later-occurring *Homo* (9, 11) [e.g., excluding *Homo habilis* sensu stricto (s.s.) (hereafter, "non-*habilis Homo*"), or *Homo ergaster*/*erectus* and later]. However, a lineage-specific size shift has not been tested alongside a general trend in a single model. Furthermore, past analyses on general trends have not accounted for phylogenetic nonindependence or intraspecific variation.

Using an expanded dataset of body mass estimates from 386 specimens across 21 taxa (Fig. 2*A*), we test for both a general temporal trend and a separate shift in body mass within *Homo*. Multiple sources of uncertainty—from body mass estimates and taxonomic classifications to phylogenetic relationships—have complicated interpretations of hominin size evolution (7–12). The choice of estimation methods and reference datasets also critically influences results (9–11). We apply Bayesian phylogenetic generalized linear mixed models (PGLMMs) to address these challenges, incorporating multiple sources of uncertainty and variation (6). Our models include random effects on phylogenetic relatedness, species classification, the anatomical region of the body mass proxy, and the reference of the mass estimate. We repeated our analyses across 1,000 phylogenies and datasets to further account for phylogenetic, taxonomic, and data uncertainty. This approach, combined with "within-group centering," also allows us to test effects within and between taxa and model evolutionary changes with improved statistical rigor (6, 14).

Results

We first examined separate within- and between-species trends in body mass through time but found no meaningful distinction between the two. The posterior distributions of within-species slopes strongly overlap with between-species slopes; their differences overlap 0 by more than 5% ($p_x > 0.05$) in 60.5% of datasets (Dataset S1). Moreover, a comparison of model fit (using Deviance Information Criteria) favors one without separate within/between-species effects in 74.7% of datasets (Dataset S1). Given this, all subsequent analyses use specimen age without separating within/between-species effects.

We find good evidence for an increase in body mass with specimen age without modeling a separate shift in *Homo* [mean slope (β) = −0.032, mean $p_x = 0.035$, $p_x < 0.05$ in 77.8% of datasets; mean conditional $R^2 = 0.469$; mean phylogenetic signal = 0.413; Dataset S1]. This translates to an increase in $\log_{10}$-scaled mass from an expected average of 1.611 (~41 kg) at 4 Mya to an expected average of 1.676 (~47 kg) at 2 Mya [mean 95% credible interval (CI) for β = −0.061, −0.003; $\log_{10}$-scaled mass increases to the present]. Phylogenetic

Author affiliations: [a]Ecology and Evolutionary Biology Division, School of Biological Sciences, University of Reading, Reading RG6 6AJ, United Kingdom; [b]Institute of Human Sciences, School of Anthropology and Museum Ethnography, University of Oxford, Oxford OX2 6PE, United Kingdom; and [c]Department of Anthropology, University College London, London WC1H 0BW, United Kingdom

Author contributions: J.D.G., T.A.P., and C.V. designed research; J.D.G. and C.V. performed research; J.D.G., T.A.P., S.W., and C.V. analyzed data; J.D.G., T.A.P., and S.W. collected data; and J.D.G., T.A.P., S.W., M.S., and C.V. wrote the paper.

The authors declare no competing interest.

This article is a PNAS Direct Submission.

Copyright © 2026 the Author(s). Published by PNAS. This open access article is distributed under Creative Commons Attribution-NonCommercial-NoDerivatives License 4.0 (CC BY-NC-ND).

[1]To whom correspondence may be addressed. Email: jacob.gardner@reading.ac.uk or c.d.venditti@reading.ac.uk.

This article contains supporting information online at https://www.pnas.org/lookup/suppl/doi:10.1073/pnas.2521732123/-/DCSupplemental.

Published June 22, 2026.

Downloaded from https://www.pnas.org by 192.76.8.203 on August 10, 2026 from IP address 192.76.8.203.

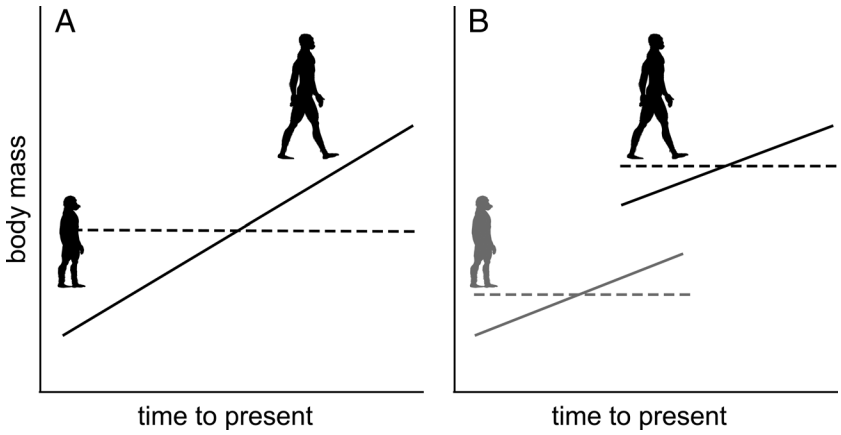


Fig. 1. Hypotheses of hominin body size evolution through time. (*A*) Body mass increased linearly through time (solid line) or did not change on average (dashed line). (*B*) Alternatively, body mass may have increased separately in *Homo* or later-occurring *Homo* (black *H. ergaster* silhouette and lines) relative to earlier hominins (gray *Australopithecus africanus* silhouette and lines), with or without a change in slope. All silhouettes are from phylopic.org (T. Michael Keesey, public domain).

signal is moderately high, underscoring the importance of accounting for phylogenetic relationships when analyzing hominin body size trends.

Accounting for a general increase in body mass, we find marginal support for a distinct size increase in all *Homo* [mean offset of *Homo* intercept (α_{Homo}) = 0.093 (95% CI = −0.005, 0.189), mean p_x = 0.044, 69.7% $p_x < 0.05$; mean conditional R^2 = 0.562; Dataset S1]. However, there is stronger evidence for a separate size increase in *Homo*, excluding *H. habilis* s.s. [mean offset of $\alpha_{non\text{-}habilis}$ = 0.111 (95% CI = 0.033, 0.187), mean p_x = 0.011, 95.8%; mean conditional R^2 = 0.582; Fig. 2 *B* and *C* and Dataset S1]. In this model, the average non-*Homo* or *H. habilis* s.s. specimen dating 2 Mya is expected to have a $\log_{10}$-scaled mass of 1.642 (~44 kg), whereas the average non-*habilis Homo* specimen of the same age is expected to have a $\log_{10}$-scaled mass of 1.753 (~57 kg). Including a separate shift in non-*habilis Homo* explains a substantial ~11% more of the variance in body mass, on average, than the model without it (difference in mean conditional R^2 or 0.582 to 0.469 = 0.113), suggesting that the most pronounced size increases occurred in non-*habilis Homo*. In this model, 72% of datasets support a trend through time [mean overall β = −0.026 (95% CI = −0.051, −0.001), mean p_x = 0.043, 72.0%; Dataset S1], but an average estimated increase through time is recovered in 100% of datasets (Fig. 2*D*). There is no evidence of a change in slope between non-*Homo* and *Homo* or non-*habilis Homo*, indicating minimal change to the overall trend through time between these groups [mean p_x = 0.323 ($p_x < 0.05$ in 0.6% of datasets) and 0.294 (2.7%) for the slope change in *Homo* and non-*habilis Homo*, respectively; Dataset S1]. There is also good evidence for a separate size increase in later-occurring *Homo*, excluding both *H. habilis* s.s. and *H. rudolfensis*, but in relatively fewer datasets (mean offset of $\alpha_{non\text{-}habilis+rudolfensis}$ = 0.103, mean p_x = 0.027, 85.3%; mean conditional R^2 = 0.574; Dataset S1). In these models, *H. floresiensis* and *H. naledi* are consistent outliers with lower-than-average body masses (Fig. 2*B* and Dataset S1).

Discussion

The literature presents conflicting support for different hypotheses of hominin size evolution: a general size increase through time (7, 12) or an increase within *Homo*, either in early *Homo* (11–13) or later-occurring *Homo* (9, 11). These hypotheses are not mutually exclusive (12) but have not previously been evaluated in a single statistical framework or while accounting for phylogenetic relationships and intraspecific variation. Our PGLMMs provide the strongest support for a separate size increase in non-*habilis* or later-occurring *Homo* (i.e., excluding *H. habilis* s.s. and *H. rudolfensis*), which coincides with increases in bipedality, carnivory, and home-range size (5). These results additionally either challenge larger body sizes as a characteristic of all *Homo*, or the inclusion of *H. habilis* s.s. in *Homo* (5, 15). However, we cannot rule out any biases in the literature in which more fragmentary postcranial specimens are assigned to species such as *H. ergaster*, and not *H. habilis*, by virtue of their larger size.

We find support for a moderate but consistently estimated size increase to the present across all hominins when accounting for a separate shift in non-*habilis Homo*. These results are partly consistent with Cope's rule (12) but overall support previous claims that body size evolution was more complex (9–12). Our detection of multiple outliers (*H. floresiensis* and *H. naledi*) further highlights this complexity (16). A general trend is largely unsupported without considering these outliers (mean β = −0.021, mean p_x = 0.126, 27.6%; Dataset S1), likely contributing to the lack of consensus around general size trends.

Many other factors may explain the lack of consensus on a general hominin size increase, including uncertainties around mass estimates. For example, De Miguel and Henneberg (7) found conflicting results when analyzing different body mass datasets, supporting a general trend only when using specimen averages. By analyzing trends across 1,000 sampled phylogenies and datasets, we found strong evidence for a separate increase in non-*habilis* or later-occurring *Homo* that is robust against phylogenetic uncertainty, size estimate uncertainty, and intraspecific variation. However, the support for a general size increase is more mixed among the datasets. Improved mass estimates and taxonomic certainty of specimens may be needed to clarify the presence or absence of a general trend. Despite concerns over using multiple body mass proxies, particularly those from upper anatomical regions, we find that it explains relatively little variation among body mass estimates when included as a random effect (mean variance explained by anatomical region = 0.032; Dataset S1). The use of anatomical region as a random effect does not distinguish estimates from proxies such as femoral head breadth or shaft breadth, of which the latter has been shown to overestimate body mass in early hominins (10, 17). However, future studies can extend our approach to distinguishing proxies from the same element.

Methods and reference samples (e.g., all hominoids or modern *Homo sapiens*) used for estimating hominin body masses also vary among studies. Multiple studies (10, 17) have raised concerns over using estimates based on body masses measured from modern human cadavers in the reference sample. Ruff et al. (10) showed that cadaveric measurements underestimated body masses calculated from stature and bi-iliac breadth by as much as 29%, which may partly explain why estimates from Grabowski et al. (9) are 25% smaller, on average, than other studies. Our primary results presented above excluded body mass estimates from Grabowski et al. (9). Including these estimates increases the support for a general size trend through time,

Downloaded from https://www.pnas.org by 192.76.8.203 on August 10, 2026 from IP address 192.76.8.203.

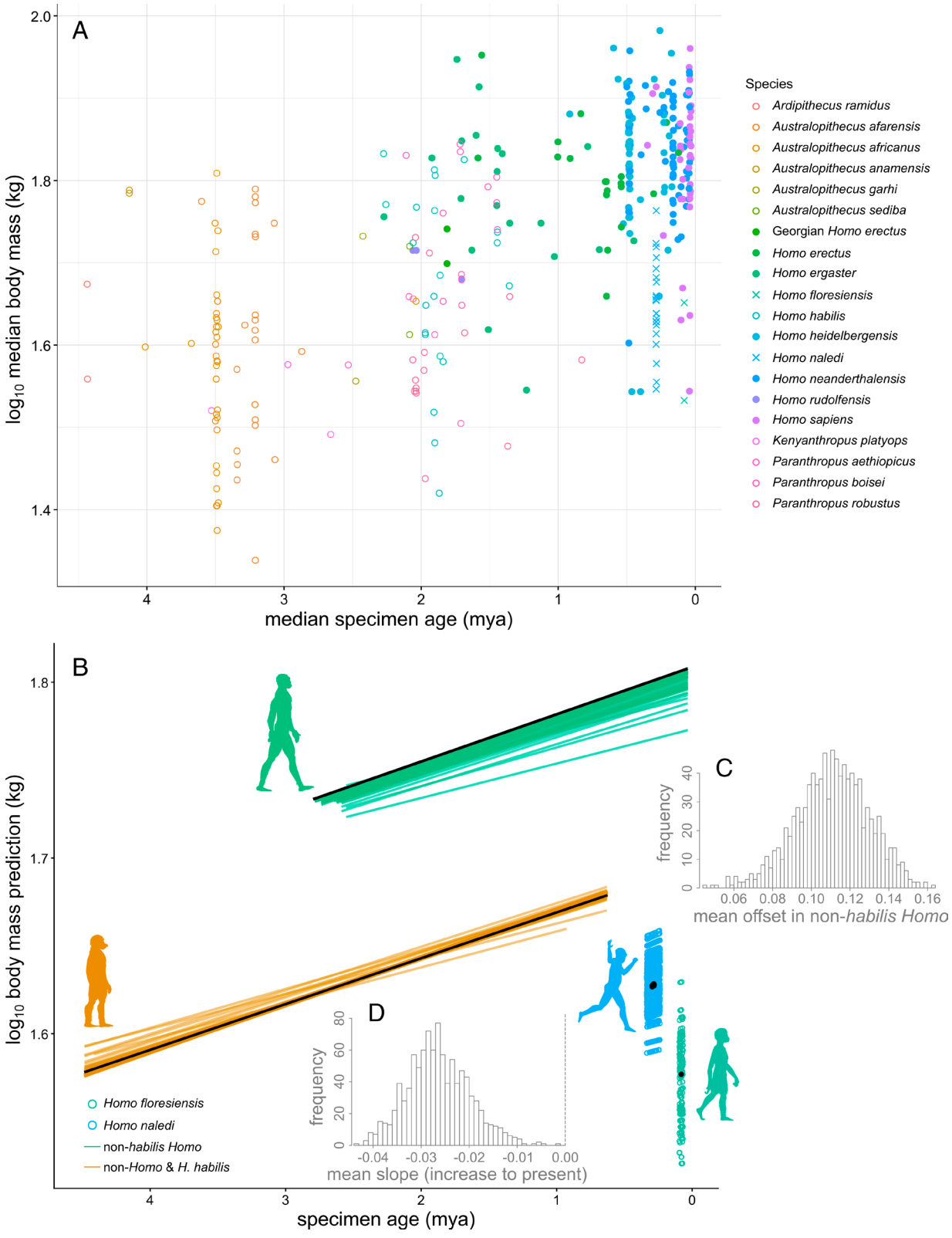


Fig. 2. (*A*) Log_{10}-scaled body mass (kilograms, kg) against age (million years ago, mya) of hominin specimens. Each point represents the median values for each specimen and is colored by the most frequently assigned species across the 1,000 generated datasets (closed circles: non-*habilis Homo* species; crosses: outliers). (*B*) Mean log_{10}-scaled body mass predictions from a random sample of 100 models, including separate intercepts for non-*habilis Homo* (*H. ergaster* silhouette) and two outliers (*H. naledi* and *H. floresiensis*, open circles). Regression lines extend beyond the data plotted above because they are based on a range of specimen ages. Black lines and points are the median predictions calculated from 1,000 models. (*C*) Distribution of mean estimated offsets in the non-*habilis Homo* intercepts from 1,000 models. (*D*) Distribution of mean estimated overall slopes from 1,000 models (negative values indicate increases to the present). All silhouettes are from phylopic.org (T. Michael Keesey, public domain).

along with a separate increase in non-*habilis Homo* [mean $\beta = -0.030$ (95% CI = −0.054, −0.005), mean $p_x = 0.021$, 87.6%; mean offset of $\alpha_{\text{non-}habilis} = 0.105$ (95% CI = 0.030, 0.178), mean $p_x = 0.012$, 96.6%; mean conditional $R^2 = 0.577$; Dataset S1]. The random effect on the reference dataset explains slightly more variation among body mass estimates, depending on which data sources are included (mean

Downloaded from https://www.pnas.org by 192.76.8.203 on August 10, 2026 from IP address 192.76.8.203.

variance explained by reference = 0.143 and 0.093 with and without estimates from ref. 9, respectively; Dataset S1). Hominin body mass estimates still vary substantially within species (11, 12). Another source of variation not factored into our analyses is sexual size dimorphism, which is more pronounced in non-*Homo* hominins (10, 17).

Overall, these findings bring clarity to a fundamental question in human evolution and show how the application of rigorous phylogenetic comparative tools can unlock patterns previously hidden in the fossil record while accounting for multiple sources of uncertainty.

Materials and Methods

Body Mass Estimates and Dataset Generation. We compiled body mass estimates (kilograms, kg) from primary and secondary literature sources (6, 9–12, 17–43), as well as temporal ranges using the latest dating information (see Dataset S2 and references therein). This includes an additional mass estimate for *Homo naledi* calculated from a regression equation with femoral cortical area (11, 44) (see entry for UW 102a-003/004 in Dataset S2). Our complete dataset includes 566 body mass estimates (n = 502 without estimates from ref. 9) for 386 specimens (n = 357 without ref. 9) across 21 taxa, including "Denisovan" specimens (Dataset S2). We limited data collection to specimens dating older than 30,000 y ago, as multiple studies have supported a recent decrease in body size (10, 18). Given its uncertain status as a hominin (45, 46), we also excluded *Sahelanthropus tchadensis* from our analyses.

When available, we preferred body mass estimates calculated from lower limb or pelvic elements over those calculated from the upper limb, axial, or cranial regions, as weight-bearing elements correlate more strongly with body mass (11). However, the reference sample used to estimate mass (e.g., all hominoids or modern *Homo sapiens*) can also affect accuracy, and some proxies may be more accurate for certain hominin species than others (10, 11). For instance, multiple studies (10, 17) have raised concerns over body mass estimates based on human cadaver specimens used in the reference sample, such as in Grabowski et al. (9), as variation in the time and conditions after death, as well as diseases acquired before death, can influence body weight. Therefore, we generated 1,000 datasets by randomly selecting a published body mass estimate for each specimen. We excluded the mass estimates from Grabowski et al. (9) in our primary dataset (Dataset S3 excludes estimates from ref. 9; Dataset S4 includes them); however, our results were consistent when we included them (Dataset S1). We further accounted for the variation in body mass owing to using proxies from different anatomical regions and using estimates from difference references by including anatomical region and the reference as additional random effects in the model (*Bayesian PGLMMs*).

Specimen ages were randomly assigned from a uniform distribution based on the temporal ranges of each specimen. Each specimen was also assigned a species based on a previously published hypodigm (6, 47). For specimens with unclear taxonomic assignments, we randomly assigned a species from a list of assignments compiled from the literature (see Dataset S2 and references therein).

Bayesian PGLMMs. We first tested for a relationship between body mass ($\log_{10}$ body mass, kg) and time (millions of years) at both intra- and interspecific levels using a combination of PGLMM and within-group centering (14). This separates specimen ages into two components: the group (or species) mean age and the within-group variability (or difference between each specimen's age and species mean). These two components were calculated for each of the 1,000 generated datasets. A more detailed description of PGLMMs and within-group centering can be found in *SI Appendix* of Püschel et al. (6). We then assessed whether we could meaningfully estimate trends within- and between-species by calculating the proportion of times when the differences in their estimates crossed a value of zero (p_x). Given that these differences overlapped with zero by more than 5% (i.e., $p_x > 0.05$), we determined that they could not be meaningfully distinguished (Dataset S1). We thus analyzed specimen age without separating within/between-species effects in all subsequent analyses.

We also consistently identified two outliers based on them having lower than average estimated body masses, accounting for specimen age: *H. floresiensis* and *H. naledi*. We determined their outlier status by including two dummy-coded variables in the model, indicating whether a specimen was assigned to one of the two outlier species (1) or not (0). For example, a specimen assigned to *H. habilis* sensu stricto (s.s.) was assigned 0 for these dummy variables.

To test for an increase in mass among *Homo* (separate intercept), we included another dummy variable indicating whether a specimen belonged to the genus *Homo* (1) or not (0). We also assessed whether *Homo* had a separate slope by including an interaction term between the dummy variable for *Homo* and specimen age. We repeated these two analyses (separate intercept and separate slope models) for non-*habilis Homo* and later-occurring *Homo* taxa (i.e., excluding *H. habilis* s.s. and *H. rudolfensis*).

Our PGLMMs account for the nonindependence of evolutionary relationships among species by including a phylogenetic variance–covariance matrix as a random effect, which models the expected covariance between species trait values based on their phylogenetic relatedness. To account for phylogenetic uncertainty, we ran our models 1,000 times, pairing one dataset with one of 1,000 sampled phylogenies from a previous Bayesian phylogenetic analysis (Dataset S5; sourced from ref. 6). We measured phylogenetic signal using a modified version of Lynch's heritability metric for nonultrametric trees (6, 48). We also accounted for the uncertainty in our mass estimates that might arise by using proxies from different anatomical regions (i.e., axial, cranial, lower limb, upper limb, or pelvic) and the use of estimates from different source references (e.g., refs. 9 and 11) by including them as additional random effects. We further quantified the relative effects that anatomical region and the reference have on body mass variation (6, 48).

We conducted all analyses using the package MCMCglmm v2.36 in R 4.4.1 (49, 50). A diffuse normal distribution centered around 0 ($\mu = 0$) with a large variance ($\sigma^2 = 10^8$) was used as a prior for fixed effects. We also used noninformative inverse-Gamma prior distributions for the random effects, with $V = 1$ and $\nu = 0$. We ran the models for 1,000,000 iterations, with a burn-in of 10,000 and a thinning interval of 500 iterations. Chains were run multiple times for each model to ensure convergence, which were assessed visually with trace plots for both fixed and random effects. We considered a model effect to be meaningful if it had a mean $p_x < 0.05$ across the 1,000 datasets. The p_x measures the proportion of the posterior distribution of model effects that crosses a value of zero. To assess the variation in support across datasets, we calculated the percentage where $p_x < 0.05$ among the datasets. We also calculated marginal R^2 (variance explained by fixed effects) and conditional R^2 values (variance explained by fixed and random effects) as measures of goodness-of-fit. An example R script for running models and calculating R^2 values and the variance explained by each individual random effect is provided in Dataset S6.

Data, Materials, and Software Availability. Study data are included in the article and/or supporting information.

ACKNOWLEDGMENTS. We would like to thank the University of Reading's Evolutionary Biology Group and Montana State University's Deep Time Biology Lab for their insightful comments. We also thank Maciej Henneberg for sharing data in the initial stages of the study. This work was supported by a Leverhulme Trust Leadership Award (RL-2019-012) to C.V.

1. R. H. Peters, *The Ecological Implications of Body Size* (Cambridge University Press, 1986).
2. W. A. Calder, *Size, Function and Life History* (Dover Publications Inc., 1996).
3. C. R. White, L. A. Alton, C. L. Bywater, E. J. Lombardi, D. J. Marshall, Metabolic scaling is the product of life-history optimization. *Science* **377**, 834–839 (2022).
4. C. Venditti, J. Baker, R. A. Barton, Co-evolutionary dynamics of mammalian brain and body size. *Nat. Ecol. Evol.* **8**, 1534–1542 (2024).
5. T. W. Holliday, Body size, body shape, and the circumscription of the genus *Homo*. *Curr. Anthropol.* **53**, S330–S345 (2012).
6. T. A. Püschel, S. L. Nicholson, J. Baker, R. A. Barton, C. Venditti, Hominin brain size increase has emerged from within-species encephalization. *Proc. Natl. Acad. Sci. U.S.A.* **121**, e2409542121 (2024).
7. C. De Miguel, M. Henneberg, Variation in hominid body size estimates: Do we know how big our ancestors were? *Perspect. Hum. Biol.* **4**, 65–80 (1999).
8. W. L. Jungers, M. Grabowski, K. G. Hatala, B. G. Richmond, The evolution of body size and shape in the human career. *Philos. Trans. R. Soc. B Biol. Sci.* **371**, 20150247 (2016).
9. M. Grabowski, K. G. Hatala, W. L. Jungers, B. G. Richmond, Body mass estimates of hominin fossils and the evolution of human body size. *J. Hum. Evol.* **85**, 75–93 (2015).
10. C. B. Ruff, M. L. Burgess, N. Squyres, J.-A. Junno, E. Trinkaus, Lower limb articular scaling and body mass estimation in pliocene and pleistocene hominins. *J. Hum. Evol.* **115**, 85–111 (2018).
11. C. B. Ruff, B. A. Wood, The estimation and evolution of hominin body mass. *Evol. Anthropol.* **32**, 223–237 (2023).

Downloaded from https://www.pnas.org by 192.76.8.203 on August 10, 2026 from IP address 192.76.8.203.

12. M. Will, A. Pablos, J. T. Stock, Long-term patterns of body mass and stature evolution within the hominin lineage. *R. Soc. Open Sci.* **4**, 171339 (2017).
13. H. Pontzer, Ecological energetics in early *Homo*. *Curr. Anthropol.* **53**, S346–S358 (2012).
14. M. van de Pol, J. Wright, A simple method for distinguishing within- vs. between-subject effects using mixed models. *Anim. Behav.* **77**, 753–758 (2009).
15. B. Wood, M. Collard, The changing face of genus *Homo*. *Evol. Anthropol.* **8**, 195–207 (1999).
16. G. D. van den Bergh *et al.*, An integrative geochronological framework for the Pleistocene So'a basin (Flores, Indonesia), and its implications for faunal turnover and hominin arrival. *Quatern. Sci. Rev.* **294**, 107721 (2022).
17. H. M. McHenry, Body size and proportions in early hominids. *Am. J. Phys. Anthropol.* **87**, 407–431 (1992).
18. C. B. Ruff, E. Trinkaus, T. W. Holliday, Body mass and encephalization in Pleistocene *Homo*. *Nature* **387**, 173–176 (1997).
19. L. C. Aiello, B. A. Wood, Cranial variables as predictors of hominine body mass. *Am. J. Phys. Anthropol.* **95**, 409–426 (1994).
20. L. R. Berger *et al.*, *Homo naledi*, a new species of the genus *Homo* from the Dinaledi Chamber, South Africa. *Elife* **4**, e09560 (2015).
21. P. Brown *et al.*, A new small-bodied hominin from the Late Pleistocene of Flores, Indonesia. *Nature* **431**, 1055–1061 (2004).
22. D. L. Cunningham, M. V. Rogers, D. J. Wescott, R. C. McCarthy, Reevaluation of the body mass estimate for the KNM-ER 5428 *Homo erectus* talus. *Am. J. Phys. Anthropol.* **170**, 148–155 (2019).
23. D. Curnoe, I. Datan, H. M. Goh, M. S. Sauffi, Femur associated with the deep skull from the west mouth of the Niah Caves (Sarawak, Malaysia). *J. Hum. Evol.* **127**, 133–148 (2019).
24. J. M. DeSilva, A. Papakyrikos, A case of valgus ankle in an early Pleistocene hominin. *Int. J. Osteoarchaeol.* **21**, 732–742 (2011).
25. F. Di Vincenzo *et al.*, The massive fossil humerus from the Oldowan horizon of Gombore I, Melka Kunture (Ethiopia, >1.39 Ma). *Quat. Sci. Rev.* **122**, 207–221 (2015).
26. H. M. Garvin *et al.*, Body size, brain size, and sexual dimorphism in *Homo naledi* from the Dinaledi Chamber. *J. Hum. Evol.* **111**, 119–138 (2017).
27. T. Harrison, "Hominins from the upper Laetolil and upper Ndolanya beds, Laetoli" in *Paleontology and Geology of Laetoli: Human Evolution in Context: Volume 2: Fossil Hominins and the Associated Fauna*, T. Harrison, Ed. (Springer Netherlands, 2011), pp. 141–188.
28. S. Hartwig-Scherer, Body weight prediction in early fossil hominids: Towards a taxon-"independent" approach. *Am. J. Phys. Anthropol.* **92**, 17–36 (1993).
29. W. L. Jungers, Lucy's limbs: Skeletal allometry and locomotion in *Australopithecus afarensis*. *Nature* **297**, 676–678 (1982).
30. J. Kappelman, The evolution of body mass and relative brain size in fossil hominids. *J. Hum. Evol.* **30**, 243–276 (1996).
31. M. R. Lague *et al.*, Humeral anatomy of the KNM-ER 47000 upper limb skeleton from Ileret, Kenya: Implications for taxonomic identification. *J. Hum. Evol.* **126**, 24–38 (2019).
32. D. Lordkipanidze *et al.*, Postcranial evidence from early *Homo* from Dmanisi, Georgia. *Nature* **449**, 305–310 (2007).
33. T. R. Pickering *et al.*, New hominid fossils from Member 1 of the Swartkrans Formation, South Africa. *J. Hum. Evol.* **62**, 618–628 (2012).
34. T. R. Pickering *et al.*, First articulating os coxae, femur, and tibia of a small adult *Paranthropus robustus* from Member 1 (Hanging Remnant) of the Swartkrans Formation, South Africa. *J. Hum. Evol.* **201**, 103647 (2025).
35. G. P. Rightmire, Brain size and encephalization in early to Mid-Pleistocene *Homo*. *Am. J. Phys. Anthropol.* **124**, 109–123 (2004).
36. C. Ruff, Body size prediction from juvenile skeletal remains. *Am. J. Phys. Anthropol.* **133**, 698–716 (2007).
37. C. B. Ruff, N. Squyres, J.-A. Junno, Body mass estimation in hominins from humeral articular dimensions. *Am. J. Phys. Anthropol.* **173**, 480–499 (2020).
38. K. L. Steudel-Numbers, M. J. Tilkens, The effect of lower limb length on the energetic cost of locomotion: Implications for fossil hominins. *J. Hum. Evol.* **47**, 95–109 (2004).
39. E. Trinkaus, C. B. Ruff, Femoral and tibial diaphyseal cross-sectional geometry in Pleistocene *Homo*. *PaleoAnthropology* **2012**, 13–62 (2012).
40. E. Trinkaus, F. H. Smith, T. C. Stockton, L. L. Shackelford, "The human postcranial remains from Mladeč" in *Early Modern Humans at the Moravian Gate*, M. Teschler-Nicola, Ed. (Springer Vienna, 2006), pp. 385–445.
41. E. Trinkaus, T. W. Holliday, B. M. Auerbach, Neandertal clavicle length. *Proc. Natl. Acad. Sci. U.S.A.* **111**, 4438–4442 (2014).
42. M. Will, J. T. Stock, Spatial and temporal variation of body size among early *Homo*. *J. Hum. Evol.* **82**, 15–33 (2015).
43. M. Will, M. Krapp, J. T. Stock, A. Manica, Different environmental variables predict body and brain size evolution in *Homo*. *Nat. Commun.* **12**, 4116 (2021).
44. J. Hawks *et al.*, New fossil remains of *Homo naledi* from the Lesedi Chamber, South Africa. *Elife* **6**, e24232 (2017).
45. R. Macchiarelli, A. Bergeret-Medina, D. Marchi, B. Wood, Nature and relationships of *Sahelanthropus tchadensis*. *J. Hum. Evol.* **149**, 102898 (2020).
46. G. Daver *et al.*, Postcranial evidence of late Miocene hominin bipedalism in Chad. *Nature* **609**, 94–100 (2022).
47. M. Dembo *et al.*, The evolutionary relationships and age of *Homo naledi*: An assessment using dated Bayesian phylogenetic methods. *J. Hum. Evol.* **97**, 17–26 (2016).
48. M. Lynch, Methods for the analysis of comparative data in evolutionary biology. *Evolution* **45**, 1065–1080 (1991).
49. J. D. Hadfield, MCMC methods for multi-response generalized linear mixed models: The MCMCglmm R package. *J. Stat. Softw.* **33**, 1–22 (2010).
50. R Core Team, *R: A Language and Environment for Statistical Computing* (R Foundation for Statistical Computing, Vienna, Austria, 2024), Deposited 2024.

Downloaded from https://www.pnas.org by 192.76.8.203 on August 10, 2026 from IP address 192.76.8.203.